Molecular Crystals and Liquid Crystals
Publication details, including instructions for authors and subscription information:
http://www.tandfonline.com/loi/gmcl16

Nucleation Phenomena in Cholestric-Nematic Mixtures Under Externally Applied Electric Fields

H. A. Van Sprang [a]
[a] Philips Research Laboratories Eindhoven, The Netherlands

Version of record first published: 17 Oct 2011.

To cite this article: H. A. Van Sprang (1985): Nucleation Phenomena in Cholestric-Nematic Mixtures Under Externally Applied Electric Fields, Molecular Crystals and Liquid Crystals, 122:1, 269-283

To link to this article: http://dx.doi.org/10.1080/00268948508074758

Mol. Cryst. Liq. Cryst., 1985, Vol. 122, pp. 269–283
0026-8941/85/1224–0269/$20.00/0/

Printed in the United States of America

Nucleation Phenomena in Cholestric-Nematic Mixtures Under Externally Applied Electric Fields†

H. A. VAN SPRANG

Philips Research Laboratories Eindhoven, The Netherlands

(*Received June 18, 1984*)

The growth of a cholesteric texture in a field-induced nematic sample is described as a nucleation process. The growth rate is found to be strongly dependent on the field at which the nucleation occurs. Expressions are derived for this dependence both at fields near the unwinding threshold and at much lower fields where the nucleation is governed by another type of process. Both processes and their physical origins are discussed.

1. INTRODUCTION

The field-induced nematic (N) state in cholesteric-nematic mixtures is known to be stable even at fields below the unwinding threshold E_{CN}^{1}. For a number of reasons, however, the N state is not infinitely stable but gradually transforms into the cholesteric C′ state. (See fig. 1 for the denomination of the various states and the corresponding director patterns.) The above described $N \rightarrow C'$ transition is rather slow immediately below E_{CN} but becomes extremely fast below E_{NC} where either C′ or C is the final cholesteric state[2–4]. Kawachi and Kogure[3] describe the growth of C both above and below E_{NC} but they give no description of the kinetics of the processes involved. Qualitatively, in their opinion, disclinations in the N state due to insufficient removal

†Paper presented at the 10th International Liquid Crystal Conference, York, 15th–21st July 1984.

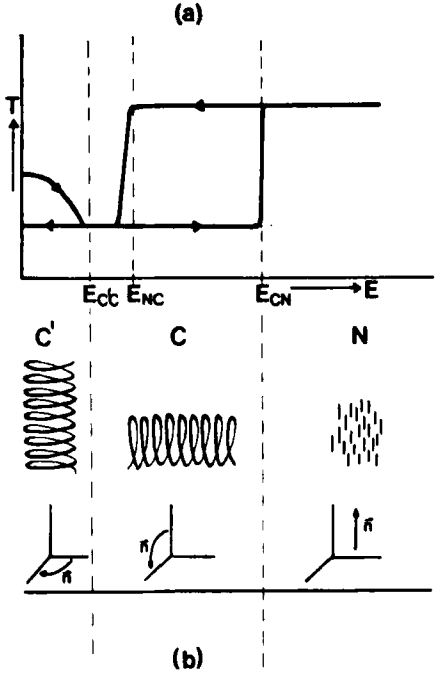

FIGURE 1 Schematic representation of a transmission-field curve for a cholesteric nematic mixture. (a) The director patterns are shown in (b) and correspond with what, for homeotropic boundaries, is commonly known as "scroll" (C'), "focal conic" (C) and "nematic" (N).

of C (at $E > E_{CN}$) act as nuclei for the C state ($E_{NC} < E < E_{CN}$). Nucleation below E_{NC} is described as a $N \rightarrow C$ transition via a temporary C' (Grandjean type) state with a double pitch. Their discussion, however, of the transitions between the various textures and the corresponding threshold fields is not quite correct.

Another approximation of the various transitions is that given by Kashnow et al.[4] who also describe the N→C transition as a nucleation process but assume the nucleation below E_{NC} to occur at the surface too. The helix structure of the C' type intermediate then grows continuously from the walls into the bulk. Recently we developed[5] a consistent model of the relevant states which occur in CN mixtures as a function of an applied electric field. The threshold fields in this description are the crossovers of total free energy curves which differ from those of Kawachi and Kogure[3] by the incorporation of surface free energy terms. The relevant aspects of our description are shown graphically in fig. 2. For $E_{NC} < E < E_{CN}$ the N state has a higher free

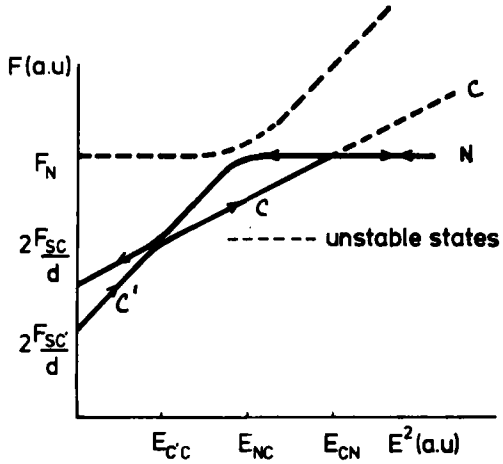

FIGURE 2 The free energy F of the three different states as a function of E^2. (For an explanation of the "avoided crossings" near $E_{C'C}$ see ref. 5).

energy than the C state but no deformation in the bulk of the sample has the right symmetry to promote the N→C transition. The only way for the transition to occur is via nucleation at the interface between N and C (if present) or at the boundaries of the sample. Below E_{NC} a bend-type deformation becomes energetically favorable and also a transition is allowed which starts in the bulk nematic phase. The transition is found to occur via an intermediate C′ state (see fig. 2). For values of $E > E_{C'C}$ the C′ state is transformed into the stable C state. If the final field $E < E_{C'C}$ the situation is more complex. As can be seen in fig. 2, two pathways are possible. Either the system follows the "upper" C′C path at $E_{C'C}$ and below $E_{C'C}$ the C′ gradually dislodges the C state, or the system directly continues via the C′ energy curve down to its final state at $E < E_{C'C}$. The latter process is only found in thin samples under fast (adiabatic) switching conditions, while otherwise the first process is found to occur.

In this paper we present a study of the time-dependence of the growth of the C state at various fields below E_{CN}. In section 2 a nucleation theory is developed which is used to analyse the experimental results in section 3.

2. NUCLEATION THEORY

Our starting point is a sample which is converted to the field induced nematic state at $E \gg E_{CN}$. Subsequently the field has been switched

to a value $E < E_{CN}$ and the replacement is studied of the field induced nematic state by its cholesteric counterpart. Microscopic inspection reveals that at various times and locations cholesteric nuclei come into existence which subsequently grow by means of a "chain branching" process. Analytical expressions for the progress α $(0 < \alpha < 1)$ of such a nucleation process have been derived by Pannetier and Souchay[6] for two cases. They show that when the nuclei grow with a branching rate constant k_2 and without interference with other nuclei, the expression for α reads

$$\alpha = qe^{k_2 t} \tag{1}$$

where q describes the conversion process from potential nucleus to growth nucleus. This seems an adequate description of the start of the nucleation. On the other hand Pannetier and Souchay show that when the initial conversion occurs rapidly and the growing nuclei do interfere with each other (termination of the growth) the progress α can be described as

$$\frac{\alpha}{1-\alpha} = e^{k_2 t} \tag{2}$$

Unfortunately neither eq. (1) nor eq. (2) describes the behaviour of our samples. The actual situation is a combination of both above-mentioned extremes and we have combined eqs. (1) and (2) to yield

$$\frac{\alpha}{1-\alpha} = qe^{k_2 t} \tag{3}$$

Our experimental data provide us with the transmission of the sample as a direct measure for the progress of the nucleation. Because the sample is fully transparent in the nematic state ($\alpha = 0$), eq. (3) must be rewritten to

$$\frac{100 - T}{T} = qe^{k_2 t} \tag{4}$$

where T is the transmission as a percentage of the difference between the transmission in the N and C state at the relevant applied field. Eq. (4) is used to obtain values for k_2 and q at various fields $E < E_{CN}$, using the experimental transmission data.

3. EXPERIMENTAL RESULTS AND THEIR EXPLANATION AS NUCLEATION PHENOMENA

All our experiments are performed at 22°C. Three samples have been studied of different thicknesses ($d = 6.6$ μm, $d = 13.1$ μm, $d = 21.3$ μm) having homeotropic boundary conditions formed by esterification of hexadecanol with an isotropically evaporated SiO_x layer. Each sample contains a mixture of E8 (BDH) + 6% CB15 ($p_0 = 2.5$ μm) as a liquid crystal. The experimental set-up is shown in fig. 3(a, b). Via a switchboard (SB) the signal of either of three generators g_i ($i = 1 - 3$) is applied to the sample during time t_i.

The transmission of the sample (S), which is taken as a measure of the progress of the nucleation, is monitored by a photomultiplier (PM) coupled to a microscope (M). The output signal of the photomultiplier is coupled to a transient recorder (TR) which is triggered at the end of either t_1 or t_2. The photomultiplier can be exchanged for a photocamera and this has been used to take some pictures of the development of the nucleation process. In order to

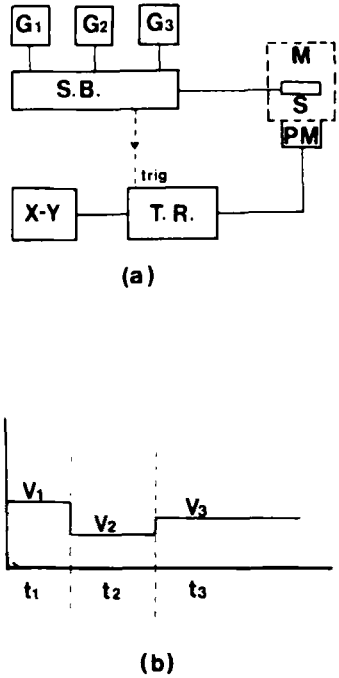

FIGURE 3 (a) Experimental set-up, and 3(b) Definition of (V_i, t_i) ($i = 1 - 3$).

TABLE I

Threshold voltages for samples of various thicknesses

d (μm)	pitch (μm)	V_{CN} (V)	V_{NC} (V)
6.6	2.5	3.6	2.0
13.1	2.5	8.9	3.9
21.3	2.5	16.4	7.2

have enough time available to expose the film it has sometimes been necessary to "freeze" the desired picture by application of another electric field so that a contrast between different states is visible for a longer time. Details are provided below for each case separately. In the rest of this section the separate samples will be characterized using their threshold voltages V_{NC} and V_{CN} rather then the corresponding fields. Voltages below threshold are then expressed in terms of $\Delta V_{CN} = (V_{CN} - V)/V_{CN}$ or $\Delta V_{NC} = (V_{NC} - V)/V_{NC}$ respectively, depending on the threshold concerned. This is based on the idea that V_{CN} and V_{NC} have the same significance for each sample and can hence be used as internal reference voltages. The V_{CN} and V_{NC} values for all samples are given in Table I.

3.1. Nucleation for $V_{NC} < V < V_{CN}$

The nucleation process in this voltage range is best illustrated by the two series of pictures fig. 4(a–d) and fig. 5(a–d) in which the time dependence of the nucleation for two different values of ΔV_{CN} for the 6.6 μm sample can be seen. The freezing process necessary to take the picture consisted in the following pulse sequence:

$$(V_i, t_i) = ((3V_{CN}, 10\text{ s}), (yV_{CN}, x\text{s}), (0, \infty)) \tag{5}$$

where, due to application of a voltage pulse yV_{CN} ($y < 1$) during x seconds, the N state transforms to C. The switching to OV transforms the remaining N to C′, which appears as the background in the photographs while the growing nuclei stay in the C state upon rapid switching to OV. This demonstrates the rapid, nonequilibrium crossing around $E_{C'C}$ as described by v. Sprang and v.d. Venne[5]. It is obvious from the figures that at the higher value of $\Delta V_{CN} = 0.42$ a circular growth is observed while the slower growth at $\Delta V_{CN} = 0.25$ leads to moon-shaped nuclei. This difference is also reflected in the higher values of x which are necessary to obtain a certain growth at $\Delta V_{CN} = 0.25$. The corresponding transmission curves for the 6.6 μm

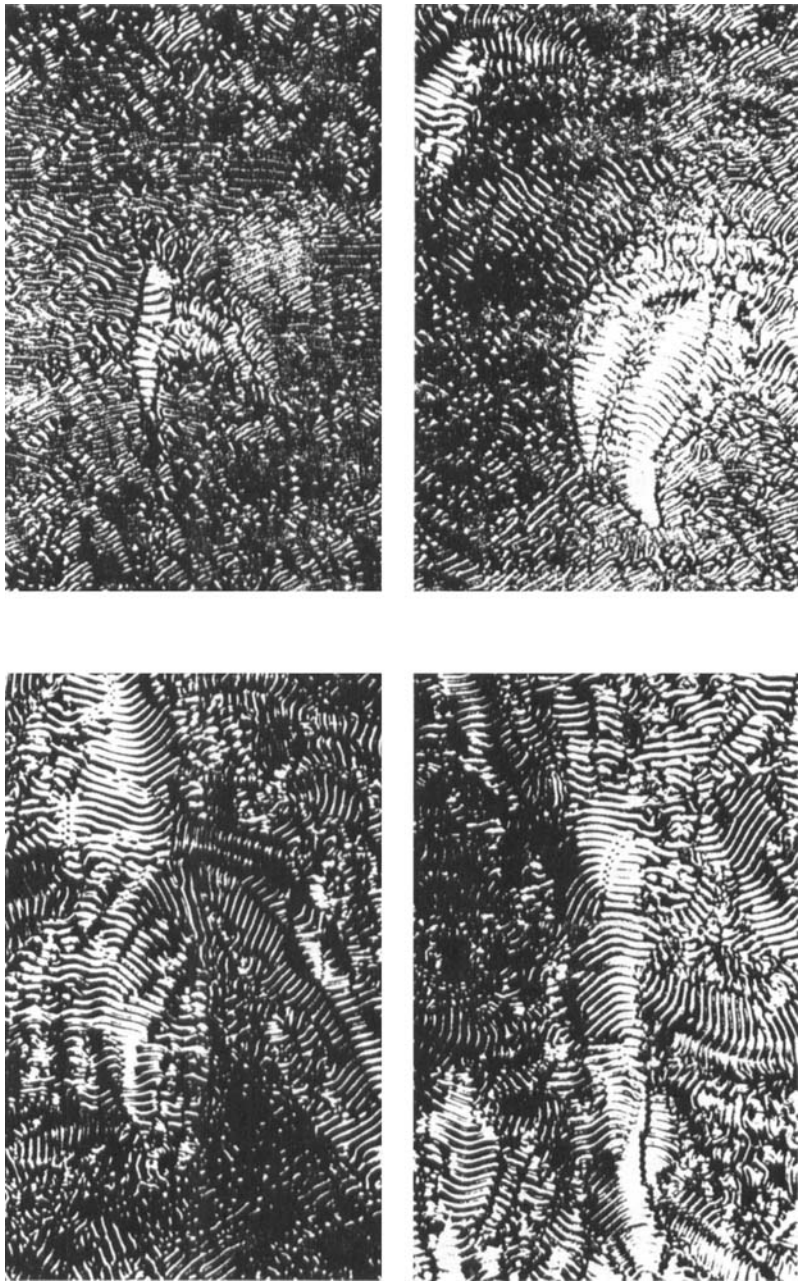

FIGURE 4 Photomicrographs of the $d = 21.3$ μm sample at $\Delta V_{CN} = 0.25$. Pictures were taken at $x =$ (a) 5 s, (b) 10 s, (c) 20 s, (d) 30 s.

TABLE II

k_2 and q vlaues for three samples of various thicknesses at specific ΔV_{CN} values.

6.6 μm				13.3 μm				21.3 μm			
ΔV_{CN}	k_2	q	r^2	ΔV_{CN}	k_2	q	r^2	ΔV_{CN}	k_2	q	r^2
0.13	0.04	0.01	1	0.14	0.07	0.01	1	0.09	0.02	0.01	1
0.18	0.07	0.01	0.99	0.20	0.10	0.01	0.99	0.12	0.04	0.01	1
0.32	0.34	0.25	0.99	0.26	0.18	0.02	1	0.15	0.07	0.01	1
				0.33	0.28	0.04	0.99	0.18	0.09	0.01	1
								0.21	0.11	0.01	1
								0.24	0.17	0.01	0.99
								0.27	0.23	0.01	1
								0.30	0.27	0.01	1
								0.33	0.34	0.01	1

and 21.3 μm samples (fig. 6(a–c)) also indicate the influence of V on the relevant time scale. The small jump at 7.2V (21.3 μm) represents V_{NC} as given in Table I. A set of such curves has been analysed in terms of eq. (5) and the results for all samples are presented in Table II where r^2 represents the coefficients of determination of the least squares adaptation procedure. As can be seen, k_2 depends strongly on ΔV_{CN} while q is much less a function of this parameter. The q values, however, are not constant over the whole range which could mean that the initial number of nuclei is also a function of ΔV_{CN}. Our data for k_2 as a function of ΔV_{CN} are fitted to the function:

$$k_2 = 0.02 - 0.21\Delta V_{CN} + 3.45\Delta V_{CN}^2 \qquad (6)$$

(with $r^2 \geqslant 0.99$) which expression is valid up to $\Delta V_{CN} = 0.35$. The experimental points and the fitted curve are given in fig. 7.

3.2. Nucleation below V_{NC}

In this range only the 21.3 μm sample has been studied extensively but the other samples show an identical behaviour. The 21.3 μm sample was more easily accessible for experiments than the other samples because of the larger difference in transmission between the studied states. Considering the curves of fig. 6c our present purpose is to study the first part of the curve before the "jump" at $V = 7.2$V. This first part is shown on another time scale in fig. 8(a) and this represents the nucleation process. The later time development is concerned with rearrangement to the configuration which is stable

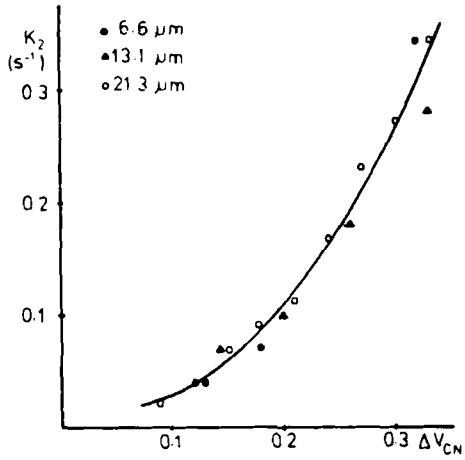

FIGURE 7 k_2 as a function of ΔV_{CN} for all three samples.

under the applied voltage. Figs. 8(b–e) show a number of photographs (between crossed polarizers) in which the nucleation process is "frozen" after different times t_2 by increasing V_3 to above V_{NC}. In our case $V_3 = 0.95\ V_{CN}$, which immediately stops the nucleation and growth as occurring below V_{NC}. It can be seen that in the time range between 50 and 70 ms the C state has fully grown over the sample. In order to adapt the experimental data to the nucleation mode we have rewritten eq. (4) as

$$\frac{100 - T}{T} = q' e^{k_2' t} \tag{4a}$$

The results for k_2 and q' for the 21.3 μm sample are shown in Table III. The values of k_2 at different V_{NC} obey the equation $k_2 = 1.3\ 10^3 \Delta V_{NC}$ when we choose V_{NC} at 8.1 V instead of the experimental value of 7.2 V. The difference between both V_{NC} values is rather large, but we do not understand its origin. As could be expected the factor q' containing information about the initial nucleation is now also dependent on V_{NC} and a full expression for the reaction rate is now found as

$$\frac{100 - T}{T} = \exp\left[(-3.9/\Delta V_{NC}) + 1.310^3 \Delta V_{NC} t\right] \tag{6}$$

which clearly shows that now both initial nucleation and growth are exponential functions of ΔV_{NC}.

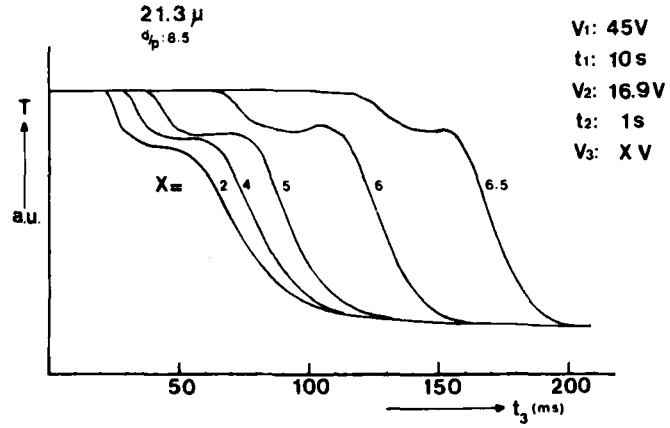

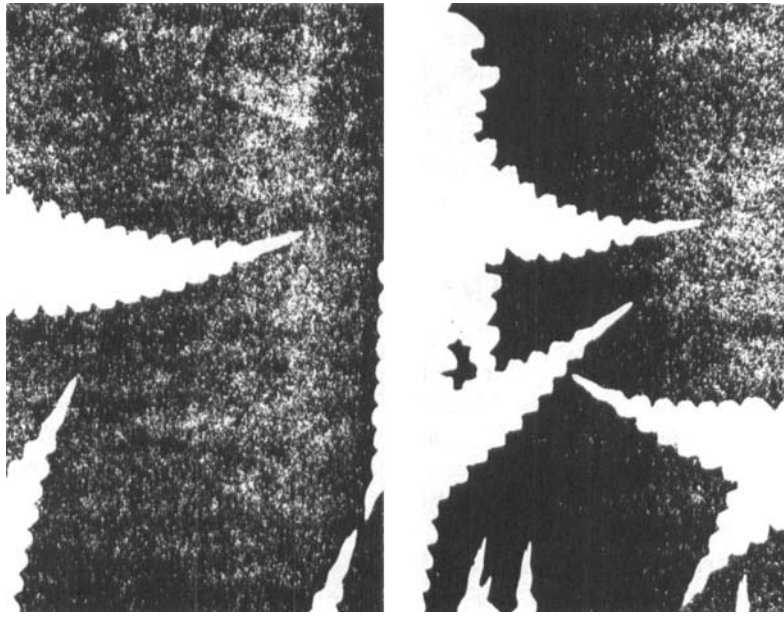

FIGURE 8 (a) Transmission curve versus time for $V < V_{NC}$ for the 21.3 μm sample (b)–(e) Photomicrographs showing the initial nucleation below V_{NC} for b) ((2 V_{CN}, 10 s), (5 V, 50 ms), (0.95 V_{CN}, 10 s)) c) ((2 V_{CN}, 10 s), (5 V, 60 ms), (0.95 V_{CN}, 6 s)) d) ((2 V_{Cn}, 10 s), (5 V, 65 ms), (0.95 V_{CN}, 2 s)) e) ((2 V_{CN}, 10 s), 5 V, 70 ms), (0.95 V_{CN}, 1 s))

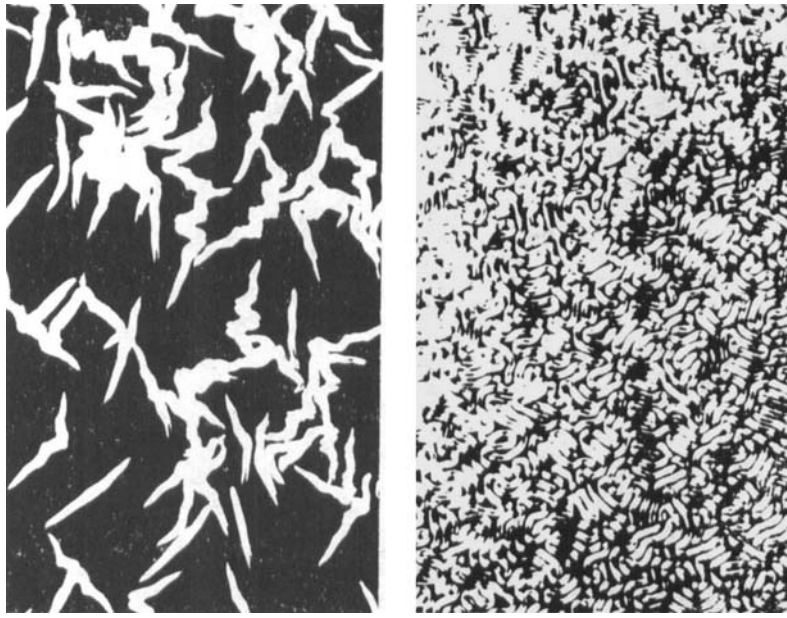

TABLE III

Values of $k_{2'}$ and q' for the 21.3 μm sample as a function of $\Delta V_{NC} = (8.1 - V)/8.1$

ΔV_{NC}	q'	$k_{2'}$	r^2
0.10	$2\ 10^{-10}$	243	1
0.26	$2\ 10^{-8}$	343	0.99
0.32	$5\ 10^{-7}$	434	0.99
0.38	$1\ 10^{-5}$	498	0.98
0.51	$3\ 10^{-4}$	642	0.99

3.3. Discussion

From the foregoing sections it is concluded that the nucleation processes in both regimes, above and below V_{NC}, differ rather considerably. Especially important is the fact that while q is almost constant for $V > V_{NC}$ ($\Delta V_{CN} < 0.35$) it has become an exponential function of ΔV_{NC} below V_{NC}. So the nucleation processes must be of a different nature above and below V_{NC}, a fact of which many previous authors seem to have been unaware[1,2,4] although it was remarked by Kawachi and Kogure.[3] We do not agree, however with their description of the differences between the processes below and above V_{NC}. From our

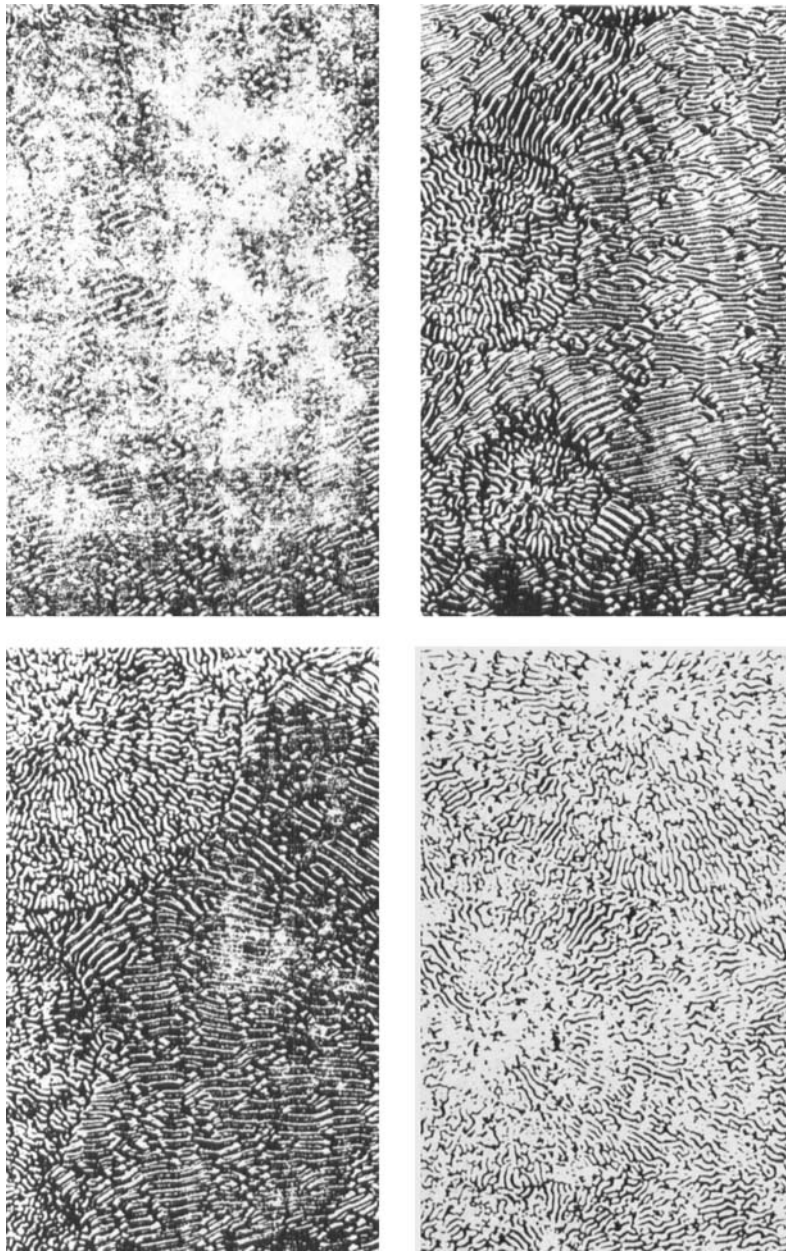

FIGURE 5 Photomicrographs of the $d = 21.3$ μm sample at $\Delta V_{CN} = 0.42$. Pictures were taken at $x =$ (a) 2 s, (b) 3 s, (c) 5 s, (d) 10 s.

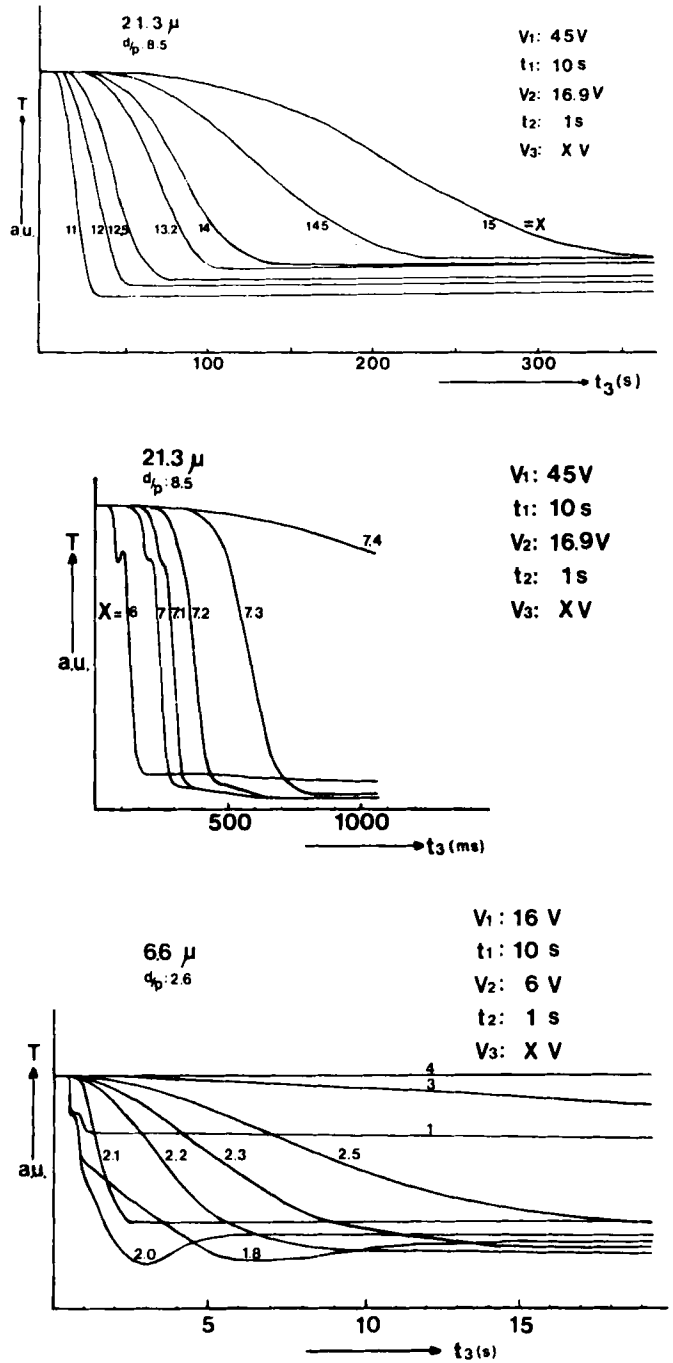

FIGURE 6 (a), (b) Transmission versus time for the 21.3 μm sample as a function of V on two different timescales. (c) Transmission versus time for the 6.6 μm sample as a function of V.

experiments it is obvious that above V_{NC} the nucleation occurs at the wall on nucleation sites which are present due to, otherwise not observable, imperfections in the orientation. Improvement of the preparation of the orienting layers has produced samples with hardly any nucleation sites at the surface[7] which are used for display applications, so apparently q is mainly dependent on the quality of the orienting layer. Once a nucleus has been formed its growth rate depends on a number of factors. In this study it has been shown that ΔV_{CN} is an important parameter. More generally, however, the liquid crystal as such and the cholesteric pitch also influence the value of the branching rate constant k_2.

Below V_{NC}, however, a bend type distortion can occur in the bulk of the sample and apparently the nucleation of a C′ type state on such distortions is much faster than the wall-induced nucleation. As a result of this change in mechanism the rate of both nucleation and growth speed up considerately below V_{NC}. The newly formed C′ type state is, however, not stable as it is formed because its helical axis is perpendicular to the glass surfaces, while in the stable C′ "scroll" state a periodic tilt of the helical axis is observed. This implies that immediately after the formation of this metastable C′ state a tranformation starts in which the helical axis becomes more tilted. For thin samples a "scroll" develops via a square-grid type perturbation as can be seen by comparing fig. 9a with a photograph of a square grid perturbation.[8] The further development of the stable C′ state is shown in figs. 9(b, c). In thicker samples the conversion to a stable state leads to a C-type state wihch is probably due to a more incoherent "tilting" of the helical axis in such samples.

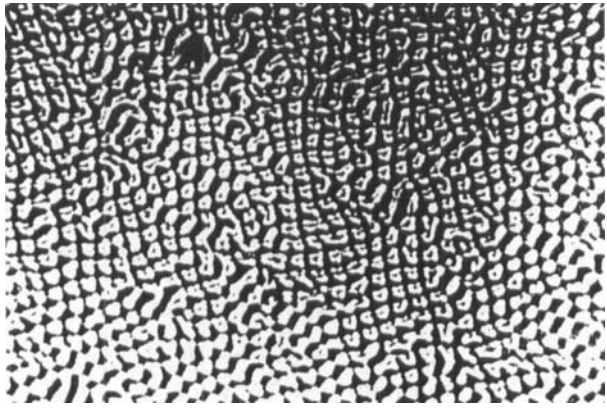

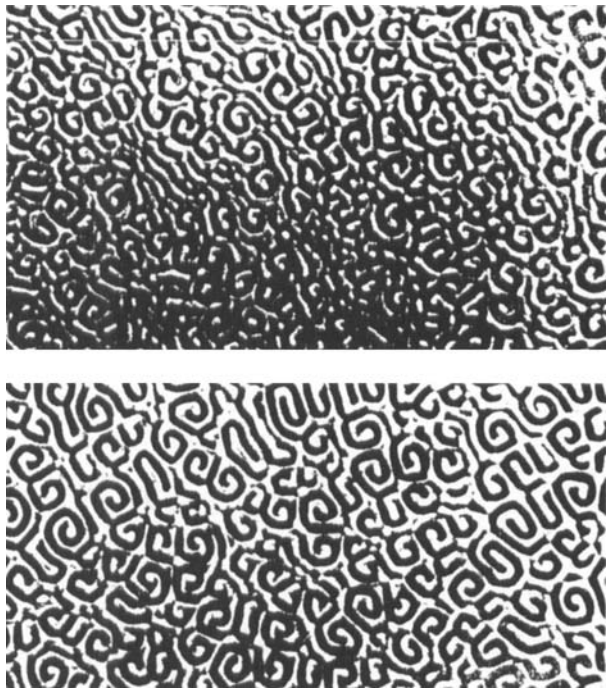

FIGURE 9 (a) Square grid pattern observed in the 6.6 μm sample upon rapid switching to 1.5 V. (b) Development of the scroll from the square grid in a after 10 s (c) after 10 min.

Acknowledgements

Thanks are due to J. P. G. M. Rijnders for performing most of the measurements and to Dr. J. L. M. van de Venne for invaluable discussions and suggestions.

References

1. W. Greubel, *Appl. Phys. Lett.*, **25**, 5 (1974).
2. S. K. Kwok and Y. Liao, *J. Appl. Phys.*, **49**, 3970 (1978).
3. M. Kawachi and O. Kogure, *Japan J. App. Phys.*, **16**, 1673 (1977).
4. R. A. Kashnow, J. E. Bigelow, H. S. Cole and C. R. Stein, "*Liquid Crystals and Ordered Fluids Vol. 4*," II p. 483. Eds. J. E. Johnson and R. S. Porter (Plenum, NY, 1974).
5. H. A. van Sprang and J. L. M. v.d. Venne, accepted for publication in *J. Appl. Phys.*
6. G. Pannetier and P. Souchay, "*Chemical Kinetics*," p. 395–410 (Elsevier, Barking, Eng., 1967).
7. H. A. van Sprang and J. L. M. van de Venne, submitted as a contribution to Eurodisplay 84, Paris, 18–20 Sept. 1984.
8. P. G. de Gennes "*Physics of Liquid Crystals*," fig. 6.17 (Clarendon Press, Oxford, 1975).